# Ultrasonic Anisotropic P-wave Attenuation of Shales under Elevated Pressures

*Liwei Ou* and Manika Prasad, Colorado School of Mines, Colorado, USA*

**Summary**

The mechanisms of ultrasonic attenuation in reservoir rock are known to be sensitive to multiple rock physical properties; this study focuses on ultrasonic experiments that measure the anisotropic attenuation in shales as function of hydrostatic confining pressure; four Eagleford and Bakken samples were measured using new experimental setup that allows measuring anisotropic acoustic properties of sample simultaneously with only one core plug. Our tests show that P-wave attenuation is sensitive to confining pressure, and attenuation anisotropy is stronger than velocity anisotropy, especially for more isotropic samples; the highly active change of attenuation with pressure supports the opinion that attenuation is a highly sensitive parameter to rock intrinsic properties. Moreover, attenuation as a function of pressure clearly suggests a two-phase attenuation mechanism exists in shale: high aspect ratio pores/microcracks closure and the related scattering attenuation on crack surfaces dominate attenuation behavior under low pressure, while at high pressure the main mechanism shifts to intrinsic attenuation caused by grain/crack friction and anelasiticity. The measured anisotropy data could be used for understanding the loss mechanisms responsible for seismic attenuation, and would benefit the development of theoretical attenuation rock physics models, as well as the interpretation of well logging and seismic surveys in shale reservoirs.

**Introduction**

Shales gas has been well-recognized as one of the most important unconventional hydrocarbon resources; due to its clay particle alignment, high aspect-ratio pores (or microcracks), organic content and bedding layers, shales are often textual anisotropic material. This anisotropy leads to the directional elastic and inelastic properties of shales, which has a major influence on the seismic and ultrasonic wave propagations when performing seismic surveys or well loggings.

Velocity anisotropy is one of the shale anisotropic properties that have been widely studied; experimentally, shale acoustic velocity is mostly measured in labs assuming a transverse isotropic media, and many interpretations on correlations between velocity anisotropy and shale petrophysical properties (Liu, 1994; Vernik & Liu, 1997; Hornby, 1998; Sone, 2012).

However, attenuation and attenuation anisotropy, which are critical for interpretation of shale physical properties, have been rarely measured in lab. In reservoir rocks, the major attenuation mechanisms could be concluded into three sections: 1) rock frame anelasticity, including static & dynamic friction between crack surface, static & dynamic friction between mineral grains, and matrix mineral inherent anelasiticy; 2) scattering attenuation due to heterogeneity and pore/crack surfaces; and 3) fluid – rock interaction, including Biot's fluid attenuation and squirt flow (Deng et al., 2009). Studies have demonstrated that attenuation has strong correlation with the saturation status and saturation fluids in rocks (Johnston and Toksoz, 1980, Best and McCann, 1994, Batzle et al.,2005), as well as flow properties including porosity and permeability (Klimentos and McCann, 1990; Rasolofosaon and Zinszner, 2002). Moreover, the attenuation and attenuation anisotropy in shales is sensitive to the rock structures including texture, heterogeneities, and existence of fractures (Prasad and Nur, 2003; Lucet and Zinszner, 1992; Carcione et al., 2012); thereby, the attenuation information of shales would be highly valuable to successful downhole and seismic interpretation of self-resourcing rocks.

This study intends to perform ultrasonic anisotropic attenuation measurements on shale samples, and discusses the attenuation mechanisms and components. To achieve this goal, a new experimental setup that allows to measure the directional acoustic velocities of shale sample under elevated pressures using only one core plug was designed and applied. Four exposed samples from Eagleford and Bakken were selected for test, and the results of measured directional P-wave velocity and attenuation at ultrasonic frequencies as a function of confining pressure are present in this paper. The P-wave attenuation anisotropies of measured samples are also quantified and discussed in this paper following the parameters defined by Prasad and Manghnani (1997).

**Methodology and Samples**

In this study, spectral ratio method (Toksoz et al., 1979) were applied in order to measure ultrasonic attenuation. The spectral ratio method measures the amplitude of samples as well as a reference with negligible attenuation; in this case, an aluminum plug is measured prior to the shale sample test as reference. The quality factor Q was calculated by the amplitude ratio between reference and sample:

$$ln\left(\frac{A_1}{A_2}\right) = (\gamma_2 - \gamma_1)xf + ln\left(\frac{G_1}{G_2}\right) \quad (1)$$

$$Q = \frac{\pi}{\gamma v} \quad (2)$$

For aluminum plug that has qualify factor Q>150,000, $\gamma_1$ is approximately 0. Thus, the value of $\gamma_2$ is the slope of amplitude ratio – frequency correlation; the quality factor of sample could be further calculated by $\gamma_2$.

To assess the velocity and attenuation anisotropy, under the assumption of TI (transverse isotropy) material, each collected sample needs to be measured in 3 directions to the bedding plane: parallel, 45 degree and perpendicular. A new one core measurement system was developed for this purpose based on Woodruff's design to simultaneously measure the acoustic and electrical anisotropies of rock samples under elevated confining pressure using only one core prepared parallel to the bedding plane(Figure 1(a)); in the new design, The core component of this improved setup is one 38.1mm inner diameter PET core jacket, which seals the core from hydraulic confining fluid, also provide base to place acoustic piezoelectric crystals. To effectively transfer pressure from confining fluid to sample, the sidewall is reduced to 0.3mm; six sets of crystals, each includes one P-wave and one S-wave crystal, are placed on sidewall as three transmitter-receiver groups, with 45-degree angle in between (Figure 1.b). All P and S wave crystals vibrate at central frequency of 1MHz.

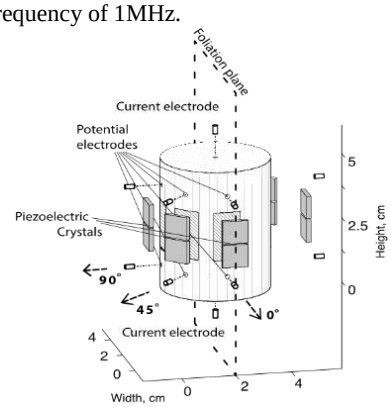


(a)

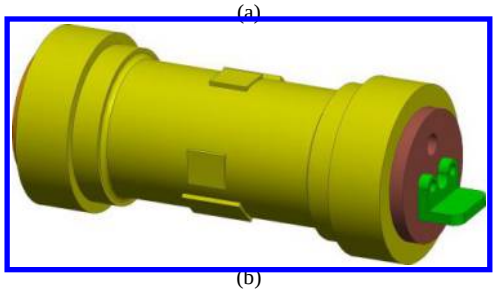

(b)

Figure 1. (a) Perspective viewpoint of anisotropic acoustic and electrical measurement system design by Woodruff et al. (2014). (b) New sample jacket design for measuring anisotropic ultrasonic velocity and attenuation under elevated pressures using only one core plug (Patent No. US62/304,479).

Before each measurement, the sample was inserted into the jacket and sealed by two polycarbonate endcaps. Pore pressure could be controlled through the pore fluid fittings on endcaps; in this study, samples were connected to the atmosphere to maintain drained conditions during pressurization. The jacket is then placed inside confined vessel, and pressurized by hydrostatic confining pressure under room temperature (≈21° C).

In our study, four samples were selected from Eagleford and Bakken for measurement. To compare the attenuation anisotropy difference between distinctive mineralogy and organic content, the two Eagleford samples (Eagleford 1,2 or EF1,2) belong to upper Eagleford chalks, and Bakken samples belong to upper Bakken shales (Bakken 1,2 or BK1,2). Eagleford samples have much higher calcite volume fraction and less clay volume and organic content. To prevent the damage from clay-swelling, air cooling method was applied in coring, also the bits were set to low revolving speed to prevent any induced fracturing during coring. After coring, the samples have not been oven dried to preserve the irreducible fluid in pore spaces.

**Attenuation as Function of Confining Pressure**

To ensure the dependability of measurement results, absolute errors in attenuation were calculated during data processing; respectively, the maximum errors for quality factor less than 15%. The P-wave attenuation as a function of confining pressure is shown in Figure 2.

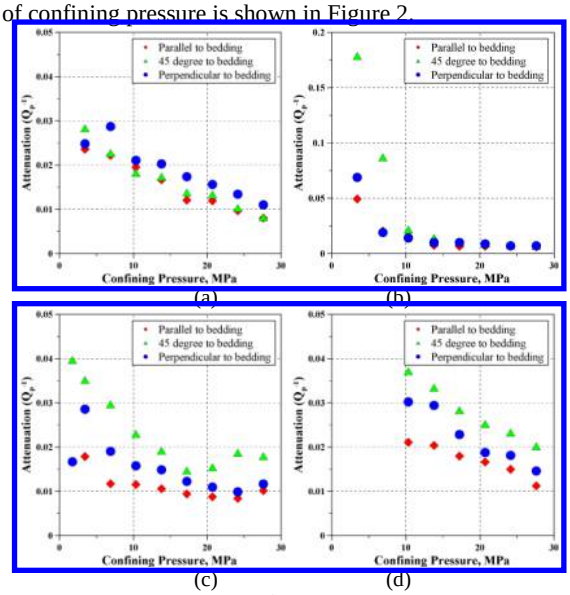


Figure 2. P-wave attenuation of sample (a) EF 1 ;(b) EF2 ;(c) BK1 ;(d) BK2 as a function of hydrostatic confining pressure, in three directions to the bedding plane: parallel (0°, red diamond), 45° (green triangle) and perpendicular (90°, blue circle). The measurement started at 0MPa and ended at 28MPa.

It is obvious that P-wave attenuation decrease with pressure conspicuously. The change in attenuation could be contributed by the high aspect ratio pores (micro-cracks) closing during pressurization, especially at initial pressure stages; however, attenuation increase rate does not show much variation between different directions to the bedding.

Among all the samples, EF2 has more cracks aligned parallel to bedding compared to other three samples as indicated by attenuation data. At the initial pressure stages, EF2 behaves a much higher attenuation at direction perpendicular to bedding under 10MPa, due to the fractures aligned at orthogonal direction; after fracture closure, the change ratios of attenuation are very similar to other samples, proving that fractures/cracks are the dominant factor of velocity and attenuation change under low pressure stages for EF2.

**Attenuation Anisotropy**

Generally, for all four samples, P-wave attenuates most when wave path is perpendicular to the bedding layer in most situations; however, the two Bakken samples have highest attenuation at 45°. This high attenuation is partly due to the scattering on the different layers, and partly due to the intrinsic attenuation.

Prasad and Manghani (1997) introduced equations to quantify the P-wave velocity and attenuation anisotropies by:

$$A_{V_p} = 200 \cdot \frac{(V_{ph} - V_{pv})}{(V_{ph} + V_{pv})} \quad (3)$$

$$A_{Q_p} = 200 \cdot \frac{(Q_{ph} - Q_{pv})}{(Q_{ph} + Q_{pv})} \quad (4)$$

For measured samples, velocity anisotropy has significantly less pressure sensitivity than attenuation anisotropy (Figure 3); moreover, the value of attenuation anisotropy is much higher than velocity anisotropy, especially in less anisotropic samples (EF2). From Figure 3(b), crack closure could be noticed from attenuation anisotropy change at 7MPa and 17.2MPa, while no such character could be found in velocity anisotropy.

With high clay content, Bakken samples has clearly higher velocity anisotropy; however, Figure 3(b) suggests that attenuation anisotropy does not have direct correlation with clay volume: the $A_{Qp}$ value of EF2 lays in between BK1 and BK2. This might imply that the microcracks and pores alignment are more dominant factor for P-wave attenuation anisotropy, compared to mineral grains alignment and related friction loss/mineral inherent anelasiticity.

**Attenuation Mechanisms – Example of Sample EF2**

Sample EF2 provides a good example for this study to analyze the attenuation mechanisms in shales. Attenuation in rocks is commonly companied by phase hysteresis (Figure 4): at low pressures, wave energy attenuation projects a phase lag on frequency domain compared to non-attenuative reference; as pressure increase, the energy loss decreases and phase shift between sample and reference is also minished.

Another observation from Figure 4(a) is the shift between different mechanisms during loading; before 10MPa, the attenuation decreases rapidly due to the improving contact between fracture and cracks; after crack closure completes, the $Qp^{-1}$ change rate decreases with pressure increase and generally get stable above 20MPa. This two-stage character indicates a switch between two mechanisms: attenuation caused by crack scattering under low pressure and intrinsic attenuation caused by grain/crack friction and anelasiticity under high pressure. The decrease in attenuation anisotropy ratio proves the existence of aligned micro-cracks effect as well: under low pressure levels, the anisotropy is considerably increased by the opening bedding-aligned cracks; as pressure increase, the crack closure leads to a more isotropic texture, thus almost eliminate the attenuation anisotropy. This trend again demonstrates the significant contribution of aligned cracks to the attenuation under low pressures.

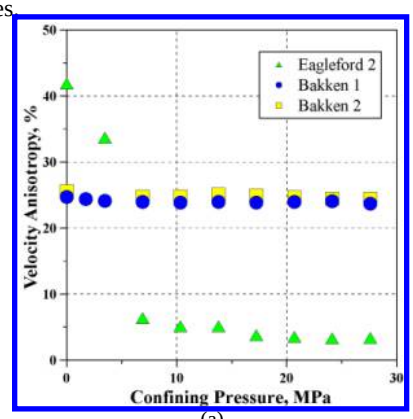


(a)

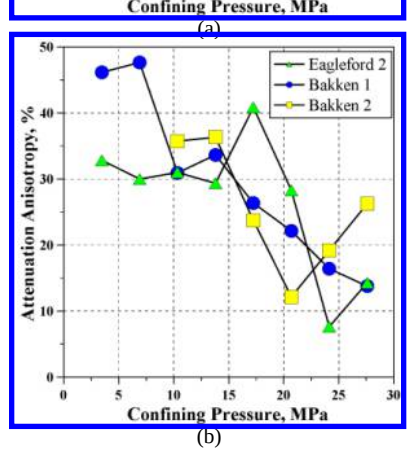


(b)

Figure 3. (a) Velocity (b) attenuation anisotropy of measured samples as function of confining pressure; The measurement started at 0MPa and ended at 28MPa.

**Conclusions**

Ultrasonic experiments at 1MHz range have been conducted on four shale samples to study ultrasonic anisotropy in shales under elevated pressures. The measurements show that P-wave attenuation behaves a high pressure sensitivity, regardless of the clay content/organic content. Also, attenuation anisotropy is more significant than velocity anisotropy, especially for samples with less velocity anisotropy.

Attenuation change with pressure clearly shows a two-stage character: the rate of attenuation increase with pressure is high at low pressures(<10MPa), and keep decrease till nearly constant at high pressures. This behavior suggests a switch between attenuation mechanisms: attenuation caused by crack scattering dominates under low pressure, and is replaced by intrinsic attenuation caused by grain/crack friction and anelasiticity at high pressures. The measured anisotropy data could be used for understanding the loss mechanisms responsible for seismic attenuation, and would benefit the development of theoretical attenuation rock physics models.

**Acknowledgements**

We would like to appreciate the financial support from Halliburton and all OCLASSH and FLUID consortium sponsors; sample support from Hess and Bakken Consortium, CSM are also acknowledged.

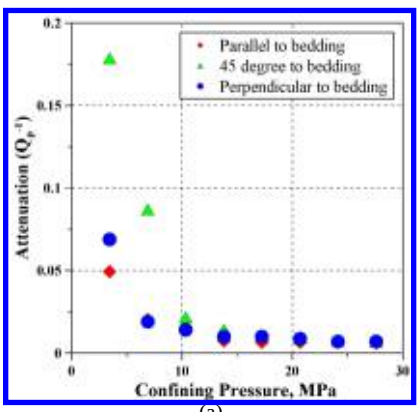


(a)

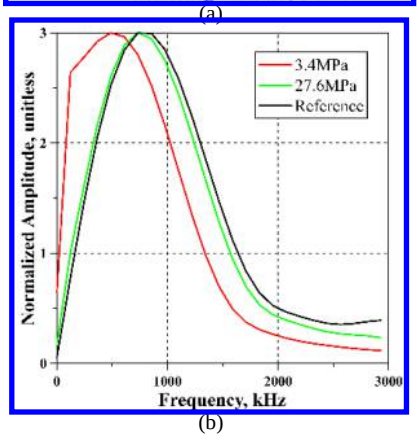


(b)

Figure 4. (a) Sample EF2 P-wave attenuation parallel (0°), 45° and perpendicular (90°) to bedding; (b) Sample EF2 0° P-wave Fourier amplitude vs. frequency at 3.4 and 27.6MPa.

**EDITED REFERENCES**

Note: This reference list is a copyedited version of the reference list submitted by the author. Reference lists for the 2016 SEG Technical Program Expanded Abstracts have been copyedited so that references provided with the online metadata for each paper will achieve a high degree of linking to cited sources that appear on the Web.

**REFERENCES**

Batzle, M., R. Hofmann, M. Prasad, G. Kumar, L. Duranti, and D.-h. Han, 2005, Seismic attenuation: Observations and mechanisms: 75th Annual International Meeting, SEG, Expanded Abstracts, 1565-1568, http://dx.doi.org/10.1190/1.2147991.

Best, A. I., and C. McCann, 1995, Seismic attenuation and pore-fluid viscosity in clay-rich reservoir sandstones: Geophysics, **60**, 1386–1397, http://dx.doi.org/10.1190/1.1443874.

Carcione, J. M., J. E. Santos, and S. Picotti, 2012, Fracture-induced anisotropic attenuation: Rock Mechanics and Rock Engineering, **45**, 929–942, http://dx.doi.org/10.1007/s00603-012-0237-y.

Deng, J., S. Wang, and D.-h. Han, 2009, The velocity and attenuation anisotropy of shale at ultrasonic frequency: Journal of Geophysics and Engineering, **6**, 269, http://dx.doi.org/10.1088/1742-2132/6/3/006.

Hornby, B. E., 1998, Experimental laboratory determination of the dynamic elastic properties of wet, drained shales: Journal of Geophysics Research: Solid Earth, **103**, 29945–29964, http://dx.doi.org/10.1029/97JB02380.

Johnston, D. H., and M. N. Toksöz, 1980, Ultrasonic P and S wave attenuation in dry and saturated rocks under pressure: Journal of Geophysical Research: Solid Earth, **85**, 925–936, http://dx.doi.org/10.1029/JB085iB02p00925.

Klimentos, T., and C. McCann, 1990, Relationships among compressional wave attenuation, porosity, clay content, and permeability in sandstones: Geophysics, **55**, 998–1014, http://dx.doi.org/10.1190/1.1442928.

Liu, X., 1994, Nonlinear elasticity, seismic anisotropy, and petrophysical properties of reservoir rocks: Department of Geophysics, School of Earth Sciences.

Lucet, N., and B. Zinszner, 1992, Effects of heterogeneities and anisotropy on sonic and ultrasonic attenuation in rocks: Geophysics, **57**, 1018–1026, http://dx.doi.org/10.1190/1.1443313.

Prasad, M., and M. H. Manghnani, 1997, Effects of pore and differential pressure on compressional wave velocity and quality factor in Berea and Michigan sandstones: Geophysics, **62**, 1163–1176, http://dx.doi.org/10.1190/1.1444217.

Prasad, M., and A. Nur, 2003, Velocity and attenuation anisotropy in reservoir rocks: 73rd Annual International Meeting, SEG, Expanded Abstracts, 1652–1655, http://dx.doi.org/10.1190/1.1817621.

Rasolofosaon, P. N., and B. E. Zinszner, 2002, Comparison between permeability anisotropy and elasticity anisotropy of reservoir rocks: Geophysics, **67**, 230–240, http://dx.doi.org/10.1190/1.1451647.

Sone, H., 2012, Mechanical properties of shale gas reservoir rocks, and its relation to the in-situ stress variation observed in shale gas reservoirs: Stanford University.

Toksöz, M., D. Johnston, and A. Timur, 1979, Attenuation of seismic waves in dry and saturated rocks: I. Laboratory measurements: Geophysics, **44**, 681–690, http://dx.doi.org/10.1190/1.1440969.

Vernik, L., and X. Liu, 1997, Velocity anisotropy in shales: A petrophysical study: Geophysics, **62**, 521–532, http://dx.doi.org/10.1190/1.1444162.

Woodruff, W. F., A. Revil, and C. Torres-Verdín, 2014, Laboratory determination of the complex conductivity tensor of unconventional anisotropic shales: Geophysics, **79**, no. 5, E183–E200, http://dx.doi.org/10.1190/geo2013-0367.1.